Study on dielectric and piezoelectric properties of 0.7 Pb(Mg1/3Nb2/3)O-3-0.3 PbTiO3 single crystal with nano-patterned composite electrode

ARTICLE *in* JOURNAL OF APPLIED PHYSICS · SEPTEMBER 2013

Impact Factor: 2.18 · DOI: 10.1063/1.4821517 · Source: PubMed

7 AUTHORS, INCLUDING:

Wei-Yi Chang
North Carolina State University
7 PUBLICATIONS **42** CITATIONS
SEE PROFILE

Wenbin Huang
North Carolina State University
23 PUBLICATIONS **81** CITATIONS
SEE PROFILE

Abhijeet Bagal
North Carolina State University
8 PUBLICATIONS **22** CITATIONS
SEE PROFILE

Xiaoning Jiang
North Carolina State University
124 PUBLICATIONS **616** CITATIONS
SEE PROFILE

JOURNAL OF APPLIED PHYSICS **114**, 114103 (2013)

Study on dielectric and piezoelectric properties of 0.7 $Pb(Mg_{1/3}Nb_{2/3})O_3$-0.3 $PbTiO_3$ single crystal with nano-patterned composite electrode

Wei-Yi Chang,[1] Wenbin Huang,[1] Abhijeet Bagal,[1] Chih-Hao Chang,[1] Jian Tian,[2] Pengdi Han,[2] and Xiaoning Jiang[1,a)]
[1]*Department of Mechanical and Aerospace Engineering, North Carolina State University, Raleigh, North Carolina 27695, USA*
[2]*H. C. Materials Corporation, 479 Quadrangle Dr., Bolingbrook, Illinois 60440, USA*

(Received 19 July 2013; accepted 2 September 2013; published online 19 September 2013)

Effect of nano-patterned composite electrode and backswitching poling technique on dielectric and piezoelectric properties of 0.7 $Pb(Mg_{1/3}Nb_{2/3})O_3$-0.3 $PbTiO_3$ was studied in this paper. Composite electrode consists of Mn nano-patterns with pitch size of 200 nm, and a blanket layer of Ti/Au was fabricated using a nanolithography based lift-off process, heat treatment, and metal film sputtering. Composite electrode and backswitching poling resulted in 27% increase of d_{33} and 25% increase of dielectric constant, and we believe that this is attributed to regularly defined nano-domains and irreversible rhombohedral to monoclinic phase transition in crystal. The results indicate that nano-patterned composite electrode and backswitching poling has a great potential in domain engineering of relaxor single crystals for advanced devices. © *2013 AIP Publishing LLC*. [http://dx.doi.org/10.1063/1.4821517]

I. INTRODUCTION

Ferroelectric materials, especially the relaxor-PT ($PbTiO_3$) crystals, have been employed for a broad range of applications such as ultrasound transducers,[1–4] sensors,[5] and actuators.[6,7] For ferroelectric compositions near the morphotropic phase boundary, the polarization can be easily rotated between different symmetries, giving rise to enhanced dielectric and piezoelectric properties.[8,9] In addition to ferroelectric composition control, piezoelectric properties in ferroelectric crystals can be enhanced using domain engineering, which is the technique to obtain certain domain configuration inside the materials by selecting crystal cuts, and/or applying electric field along one axis, creating a set of domains in which the polarization vectors are oriented to minimize their angles to the poling direction.[10] Based on the domain engineering, relaxor-PT single crystals with the composition near morphotropic phase boundary and ⟨001⟩ cut could show ultrahigh piezoelectric coefficients and electromechanical coupling factors (e.g., $d_{33} > 2000$ pC/N and $k_{33} > 0.9$), far outperforming the state-of-the-art $Pb(Zr_xTi_{1-x})O_3$ ceramics.[11–15] It has been reported that relaxor-PT single crystals exhibit a hysteresis-free strain response, which is related to the engineered domain configuration.[16]

Apart from engineered domain configuration, domain wall engineering using patterned electrodes or special poling process could also be adopted to increase the piezoelectric properties of relaxor-PT crystals by decreasing domain sizes (or increasing domain wall density) due to the extrinsic contribution from the domain wall motion.[17] Urenski *et al.* reported that the periodic domain structures can be successfully induced in $KTiOPO_4$ single crystal by patterning electrodes.[18] For [111] oriented barium titanate (BT) single crystals, Wada *et al.* induced finer engineered domain configurations by patterning electrode with gold strip line of 3 μm width per 6 μm spacing. In comparison with the 5 μm minimum domain size achieved with whole plane electrode, crystals with patterning electrodes exhibited a gradient domain sizes from 3 μm to 8–9 μm and showed a high d_{31} value of -243.2 pm/V.[19] Recently, Yamashita *et al.* reported that 0.7 $Pb(Mg_{1/3}Nb_{2/3})O_3$-0.3 $PbTiO_3$ (PMN-PT) with composite electrodes consisting of randomly distributed Mn oxide nano-islands and Au showed d_{33} increase of almost 40%.[20] Oxide nano-islands were fabricated through heat treating a spin-coated sol-gel manganese oxide layer. However, the size of nano-islands is uncontrollable and not uniform. It is difficult to distinguish the effects of various factors. When conventional poling method is adopted, which provides a voltage ramping to a value and lasting for several minutes, domain nucleation would start at the electrode edges and have a tendency to widen along the transversal direction as growth proceed. For short period domain broadening results in domain merging, thus limiting the production of the short-pitch domain patterns. Also, an internal field due to nonstoichiometric point defects leads to axial anisotropic coercive field, resulting in spontaneous backswitching upon abrupt removal of the external field.[21,22] In order to overcome these drawbacks of conventional poling technique, backswitching poling with designed short-period waveform was applied to grow periodic domains in ferroelectric materials with micro scale pattern on the surface.[23,24] Preceded by a low voltage stage when backswitching occurs, an additional stabilization stage applying external voltage larger than the instantaneous value of the decaying voltage can terminate backswitching and stabilize domains. Shur *et al.* successfully observed the formation of micro-domains in lithium niobate crystal by employing backswitching poling method to the patterned NiCr stripe electrode structure with 1.5 μm width.[23,24]

a)Author to whom correspondence should be addressed. Electronic mail: xjiang5@ncsu.edu.

In this paper, nanolithography based composite electrode fabrication was studied to investigate the effect of patterned nanoscale electrode and poling scheme on dielectric and piezoelectric properties of PMN-PT single crystals. There exist a few approaches such as e-beam patterning, focus ion beam milling, and nano-imprint lithography to obtain electrode nanostructures on ferroelectric materials. In relatively large scale, however, these methods are time consuming and expensive. On the other hand, Lloyd's mirror interference lithography[25] (LIL) is an effective technique for fabricating grating structures, as it provides relatively large exposure area.[26] In order to fabricate the controllable electrode size and higher density of electrodes, in this study, we used LIL to fabricate composite nano-electrode on PMN-PT and adopted backswitching poling method to engineer domain walls and domain sizes. The paper proceeds with the following structure. First, the fabrication process of nano-patterned composite electrode on PMNT crystals will be described in detail. Conventional and backswitching poling methods will be introduced. Second, measurement results of piezoelectric properties for the crystals with different electrode type and poling condition will then be present and compared with each other. The mechanism of property enhancement induced by nano-patterned electrode and backswitching poling technique will be explained in domain engineering aspect. Finally, the conclusion will be present along with our future work.

II. EXPERIMENT

A. Nano-patterned composite electrode fabrication

Four PMN-PT single crystal plates from the same batch with dimension of 20 mm × 20 mm × 0.6 mm were prepared with one side polished for fabrication of nano-composite electrode. The processes of generating manganese (Mn) nano-pattern (nano-grating) on a single-crystal PMN-PT substrate are illustrated in Fig. 1. LIL system was used to create a one-dimensional array photoresist pattern over an area of $2 \times 2\,cm^2$ using a 325 nm ultraviolet (UV) laser. PMN-PT substrate (Fig. 1(a)) was first coated with an antireflection layer (ARC, Brewer Science i-CON-16) and a thin layer of photoresist (Sumitomo PFI-88A1/2) with the thickness of 95 and 200 nm (Fig. 1(b)), respectively. The intensity pattern recorded by the photoresist has a 1D grating structure with a period $\Lambda = \lambda/(2\sin\Theta$, where Θ is the incident angle and λ is the wavelength of UV light). After photoresist exposure and development (Fig. 1(c)), reactive ion etching (RIE) was utilized to etch through the ARC (Fig. 1(d)) to expose the PMN-PT substrate underneath. A Mn layer with thickness of 50 nm was then deposited on the PMN-PT wafer with nano-structured photoresist through electron-beam evaporation (Fig. 1(e)). The lift-off of Mn was implemented by using (Fig. 1(f)) RCA clean (5:1:1 water: H_2OH:NH_4OH) to dissolve and remove the positive photoresist and residual ARC layer (Fig. 1(g)). After lift-off, Mn nano-grating is the only layer left on the PMN-PT substrate. Heat treatment was then employed to oxidize and shrink the Mn nano-grating at 800 °C for 3 h in air. Lastly, a Ti/Au layer with thickness of 10 nm/100 nm was deposited onto the surfaces of the samples on both sides (Fig. 1(h)).

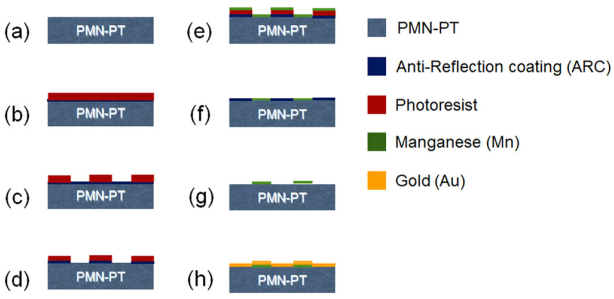

FIG. 1. Schematic of fabrication of Mn nanograting on PMN-PT substrate. (a) PMN-PT with polished surface. (b) Spin coat the ARC and photoresist with 95 and 200 nm, respectively. (c) Expose by LIL system. (d) Etch the exposed ARC part by RIE. (e) Deposit the Mn layer with 50 nm. (f) Remove the residual photoresist by the liftoff process. (g) Remove the ARC layer by RCA clean. (h) Deposit gold as an electrode.

B. Poling methods

For poling study, PMN-PT samples were poled by two methods: conventional and backswitching method. The conventional poling is to apply a constant electric field of 10 kV/cm for 5 min at room temperature. The applied electric field is significantly higher than the coercive field ($E_c = 2.5$ kV/cm).[27] The samples were dipped in the silicon oil to prevent the breakdown of air. The backswitching method involves applying an electric field with a designed waveform, as shown in Fig. 2. Similar with the technique used by Shur *et al.*,[24] a high-voltage pulse produced an electric field with the amplitude of 10 kV/cm to initiate the domain motion. During an appended low voltage stage, spontaneous backswitching occurs. Then, a stabilization stage (4 kV/cm) is added to terminate this spontaneous domain reversion and stabilize the

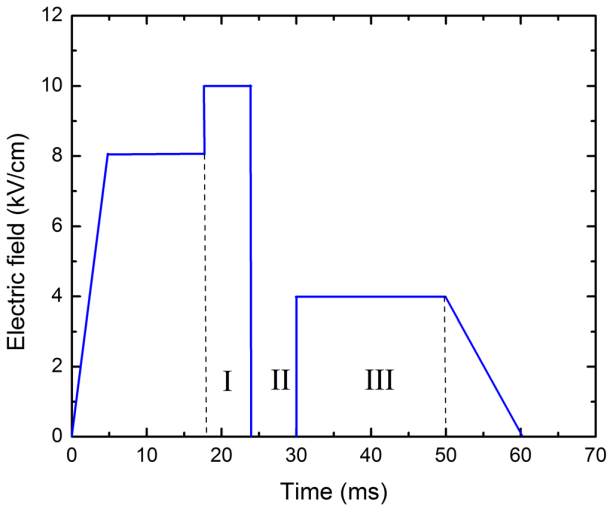

FIG. 2. Poling voltage waveforms for backswitching process. The pulse is added to prevent spontaneous domain reversion to the original configuration (backswitching process) after removing of the poling field. I (high field): The switching from the single domain took place, II (low field): The backswitching occurred at this step, and III (stabilization): Nano-domain structure developed during backswitching.

domains. Total period of a cycle is 60 ms. Other external conditions were set the same for all samples.

C. Properties measurement

Capacitance and dissipation factor of all prepared samples were measured at 1 kHz using an impedance analyzer (Agilent 4092A). The temperature dependences of dielectric properties were characterized at the same frequency using the same measuring system within the range of 25 to 185 °C. Piezoelectric constant d_{33} was measured at room temperature using a system comprising of two main components: a Trek-2220 high voltage amplifier and a linear variable differential transformer (LVDT) for displacement monitoring. In order to better understand the characteristics of PMN-PT with and without nano-composite electrode and under pulse or conventional poling, we designed experiments and processes samples with different treatments: conventional electrode (blanket Ti/Au on both sides) with conventional poling method (sample A), nano-composite electrode with conventional poling method (sample B), conventional electrode with backswitching poling method (sample C), and nano-composite electrode with backswitching poling method (sample D).

III. RESULTS AND DISCUSSION

A. Fabricated nano-composite electrodes

Nano-patterned Ti/Au-Mn nano-composite electrodes were fabricated following the process shown in Fig. 1, including LIL nano-lithography, sputtering thin film coating of Mn and T/Au, lift-off, and thermal annealing process. Fig. 3 shows the field emission scan electronic microscope (FE-SEM) pictures of the fabricated Mn nano-grating. According to the formula, $\Lambda = \lambda/(2n \sin\Theta)$, the precise pitch of 200 nm was obtained with an incident angle of 54°, as shown in Fig. 3(a). Figs. 3(b) and 3(c) show the topography SEM images of the wafer after the Mn deposition and lift-off process, respectively. After the heat treatment, the Mn nano-grating lines shrank and aggregated into isolated nano-islands along the nano-grating lines, which can be observed in Fig. 3(d). After the fabrication

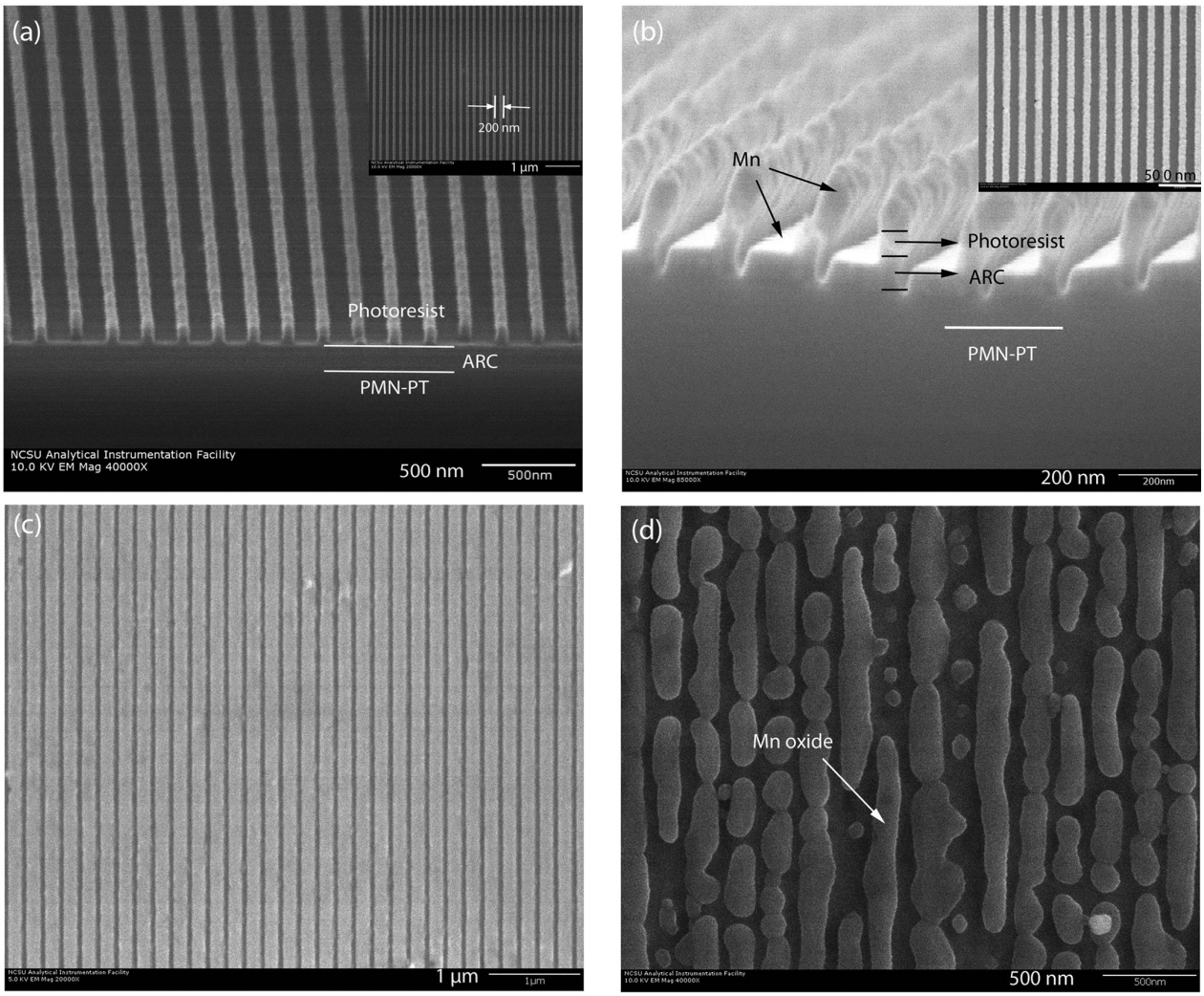

FIG. 3. The field emission scan electronic microscope (FE-SEM) images of the Mn nano-grating. (a) Nano-grating with precise pitch ($\Lambda = 200$ nm). (b) Topography images of the Mn deposition. (c) Mn nano-grating after the lift-off process. (d) After heat treatment, Mn nano-grating shrinks into nano-islands.

of nano-patterns, the traditional and backswitching poling method were introduced to pole the prepared samples.

B. Dielectric constant calculation

The dielectric constant (ε) was calculated by using the measured capacitance (C) and sample dimension ($\varepsilon = C \times d/(A \times \varepsilon_0)$, where A is the effective area of the electrode, d is the distance between the top and bottom electrodes, and ε_0 is the permittivity of vacuum). Determination of A can be implemented by finite element analysis. COMSOL was used to simulate the electrical field distribution in PMN-PT with nano-composite electrode. An insulated nano-grating layer with a pitch of 200 nm and a height of 50 nm was created to model the MnO layer. The relative dielectric constants of insulated layer and PMN-PT are 5 and 4000, respectively. The bottom side of the sample is grounded, and a certain amount of charge is assigned to the top surface. Electric field and voltage distribution can be obtained through simulation, as shown in Fig. 4. Electric field shows some singularity near the nano-composite layer while becomes uniform beyond 100 nm. Based on the capacitance of the sample which equals the division of assigned charge amount and measured voltage, the effective electrode area can be given as $A_s = C_s \times d_s/(\varepsilon_r \times \varepsilon_0)$, where C_s is the capacitance form the simulation, d_s is the thickness of the PMN-PT sample, ε_r is 4000, and ε_0 is the vacuum permittivity which is 8.854×10^{-12} (F/m). The calculated electrode area is similar to the whole blanket area, indicating that the existence of nano-composite layer would not change the charge storage capability significantly.

C. Dielectric and piezoelectric characterization

With the measured capacitance, the whole surface area, instead of only the area that is in direct contact with electrodes, was used for dielectric constant calculation. To measure the d_{33} of all samples, a triangle wave with voltage varying from 0 V–400 V-0 V within 10 s was applied to samples. The displacement at every 0.4 V increment was recorded and showed good linearity with voltage. The linear fit slope was thus the measured piezoelectric constant. Piezoelectric constant was calculated by dividing the measured displacement by voltages. Table I shows the dielectric constant and piezoelectric properties of samples A–D. Each sample type consists of four smaller sample pieces (5 mm × 5 mm, diced from the 20 mm × 20 mm crystal plates), and the dielectric and piezoelectric measurements of these samples were repeated many times in the time span of 5 days. Results exhibited little scattering and averaged values of 5 data points (each from one day) are presented here. The effect of backswitching poling method in improving the electromechanical properties of PMN-PT can be observed by comparing dielectric and piezoelectric properties of samples C and D with those of samples A and B. The backswitching poling process has been considered as an effective method to enhance generation of nano-domain structures which includes several distinguishable stages of domain evolution.[23,24] During the backswitching poling, the process starts with the formation of new domains at the surface along the nano-electrode edges due to the field singularities caused by the fringe effect. In other words, the nano-grating composite electrode on the surface of PMN-PT can provide periodic nucleation sites. The domains then grow and propagate through the wafer forming the laminar domains. Domain broadening along the transversal direction causes domain coalescence.[28] Backswitching poling process removes the voltage shifts, but conventional poling process leads to large internal fields and high frozen-in polarization,

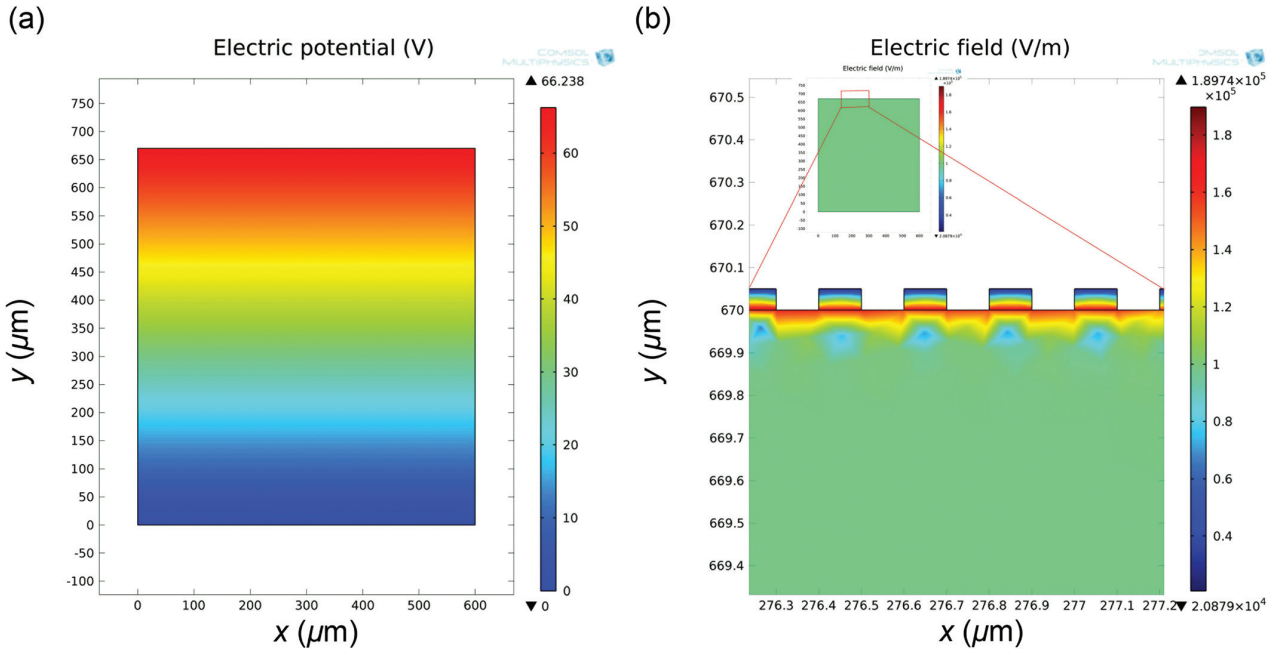

FIG. 4. The finite element simulation results of (a) electric potential in PMN-PT with nano-composite electrode and (b) electric field distribution in enlarged area near the nano-composite electrode surface (inset shows the whole distribution).

TABLE I. The dielectric and piezoelectric properties of the samples with different fabrication and poling processes: Conventional electrode with traditional poling (A), nano-composite electrode with traditional poling (B), conventional electrode with backswitching poling (C), and nano-composite electrode with backswitching poling (D).

Properties	A	B	C	D
Dielectric constant ε before poling	3550	3163	3059	2965
Dissipation factor tan δ before poling (%)	3.82	3.82	3.81	3.74
Dielectric constant ε after poling	6213 ± 100	7528 ± 70	6789 ± 60	7802 ± 80
Dissipation factor tan δ after poling (%)	0.49	0.58	0.46	0.57
Piezoelectric constant d_{33} (pm/V)	1600 ± 25	1620 ± 20	1850 ± 30	2040 ± 20
Electromechanical coupling factor k_t (%)	59.93	58.97	56.84	59.36

which induces domain reversion after the abrupt removal of the external electric field. Table I does not show obviously different dielectric constant and d_{33} values of sample A and B, which are samples with conventional poling. The reason possibly lies in that the electric field distributions and domain evolution in sample A and sample B are similar. Even though nano domain nucleation will arise due to the fringe effect of nano-patterned composite electrode, they will either merge during propagation or back switch once the electric field is removed. On the other hand, sample D has higher dielectric constant (7802) and d_{33} (2040 pm/V) value than those of sample C, to which backswitching poling has been both applied. We suppose that the stabilization field in backswitching poling method could avoid the spontaneous domain reversion, and repeated short period electric pulses could assist the alignment of nano domains during propagation. Then the regular and defined nano-domains can be obtained, thus increasing the piezoelectric and dielectric properties of PMN-PT. Specifically, d_{33} value and dielectric constant of sample D is 27% larger and 25% higher than those of the sample A, respectively.

Piezoelectric activity is known to be attributed to extrinsic effect (irreversible domain wall motion) and intrinsic effect (reversible domain distortion due to polarization rotation). The extrinsic effect generally contributes to the piezoelectric response in polycrystalline ceramics, which is accompanied with large hysteresis and dielectric loss. The ultrahigh piezoelectric properties in relaxor-PT single crystals have been theoretically attributed to polarization rotations between rhombohedral (R) to tetragonal (T) phases through monoclinic (M) or orthorhombic (O) symmetries. Crystals studied in this paper have the composition near the R/O morphotropic phase boundary and lie in R symmetry at room temperature. When electric field is applied to the (001)-cut crystal, R-M_A-M_C-T transition sequences will happen, where M_A and M_C are two types of monoclinic phases. Using *in suit* high energy X-ray/neutron and polarized light microscopy, it has been demonstrated that crystal would have a small fraction of M domains left after the removal of a relatively low electric field, which indicates that the R-M_A-M_C transition is irreversible.[29] Guo *et al.* observed an enhancement of the piezoelectric coefficient d_{33} in the similar crystals as poling field increase, from ~1550 pC/N with $E_{poling} = 10$ kV/cm to ~2500 pC/N with $E_{poling} = 30$ kV/cm.[30] They proposed that the M_A distortion should be responsible for the high piezoelectric response for crystals in rhombohedral composition region. Through the analysis of a theoretical model, Viehland *et al.* proposed that the monoclinic phase is an adaptive mixed state, which is formed by fine tetragonal micro-domains with very low domain wall energy. They thought the observed high piezoelectric activity is largely caused by 90° domain wall motion.[31]

The mechanism of piezoelectric effect enhancement induced by nano-composite electrode and backswitching poling can be further confirmed by the dielectric constant measurements, as shown in Fig. 5. Dielectric results of four crystals all show two weak peaks before a broad peak, which represents that the crystals underwent a $R(M)$-$M(R)$-T-C transition sequences ("$R(M)$" manifests that dominant R domains coexist with a smaller fraction of M domains), thus validating the existence of monoclinic phases after poling. The Curie temperatures of the samples are about the same at 150 °C. Sample A with conventional electrode and traditional poling exhibits a dielectric constant of 6213 at room temperature and about 20 000 at $T_{rm} = 103$ °C (R-M phase transition temperature). On the other hand, the dielectric constant of sample B with nano-structured electrode and traditional poling is 7528 at room temperature and increases up to about 24 500 at $T_{rm} = 108$ °C. The dielectric constant enhancement in sample B, in comparison with that of sample A, is likely resulted from the nanostructured Mn/Au composite electrode. Sample C with conventional electrode and backswitching poling

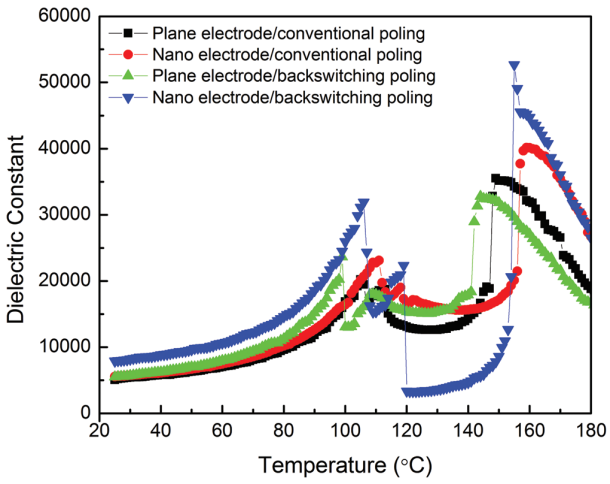

FIG. 5. Dielectric constants as functions of temperature for ⟨001⟩ oriented PMN-PT crystals under different treatments (1 kHz): bare PMN-PT with conventional poling (A), nano-composite electrode with conventional poling (B), bare PMN-PT with backswitching poling (C), and nano-composite electrode with backswitching poling (D).

exhibits a dielectric constant of 6789 at room temperature and about 23 000 at $T_{rm} = 101\,^{\circ}\mathrm{C}$. The dielectric constant of sample D is 7802 at room temperature and increases up to about 32 000 at $T_{rm} = 105\,^{\circ}\mathrm{C}$. The leftmost peak represents R-M_A transition, and the middle peak is a two-step in nature, corresponding to a transition from the M_A to T with an intermediate M_C phase.[32] The dielectric constant at temperatures ranging from the middle peak to the rightmost peak shows a low valley compared with the dielectric constant at other temperatures. It is well-known that the dielectric constant along the spontaneous polarization (P_s) direction for perovskite ferroelectrics is much smaller than that along other directions. This confirmed that the ⟨001⟩ oriented crystal has transited into T phase in this temperature range. Comparison between sample C and D with sample A and B demonstrates that backswitching poling could generate more abrupt ferroelectric-ferroelectric phase transition peaks. Similar phenomenon could be observed by comparing sample A and C with B and D, which is attributed to nano-composite electrode on the crystals. Sharper phase transition peak corresponds to larger fraction of monoclinic phases after poling, thus leading to the enlargement of piezoelectric coefficient as suggested earlier. On the other hand, nano-composite electrode and backswitching poling method employed here could create nanosize domains inside the crystal. Decreased domain size and domain wall energy could facilitate the formation of monoclinic phase during poling process.[33] In addition, increased domain wall densities in the crystals could further improve the piezoelectric coefficient through extrinsic contribution from the domain wall motion.

IV. CONCLUSIONS AND FUTURE WORK

In summary, electrode pattern and backswitching poling techniques were adopted to improve the piezoelectric response in [001] poled PMN-PT single crystals. Nano-grating Mn/Au composite electrode fabricated using interference lithography and backswitching poling yielded 27% increase of d_{33} and 25% increase of dielectric constant. Due to the ease of large size fabrication, interference lithography based fabrication of nano-composite electrode suggests a potential avenue for enhancing the piezoelectric activity in relaxor single crystals for advanced electromechanical devices. In the future, piezoelectric force microscope will be employed to directly observe the existence of nano domains induced by nano-composite electrode and backswitching poling. Percentages of different polarization symmetries will be quantified by polarized light microscopy with the aim to confirm the large amount of monoclinic phase transformation. Mechanism behind nano-composite electrode associated phase transformation will be further analyzed.

ACKNOWLEDGMENTS

This material was based upon work supported by, or in part by, the U. S. Army Research Laboratory and the U. S. Army Research Office under Contract/Grant No. W911NF-11-1-0516, in part by National Science Foundation under Grant No. CMMI-1068345, and in part by NIBIB of National Institutes of Health under Grant No. R01EB015508.

[1]J. Chen and R. Panda, Proc.-IEEE Ultrason. Symp. **1**, 235–240 (2005).
[2]W. Hackenberger, J. Luo, X. N. Jiang, K. A. Snook, P. W. Rehrig, S. J. Zhang, and T. R. Shrout, "Recent developments and applications of piezoelectric crystals," in *Handbook of Advanced Dielectric, Piezoelectric and Ferroelectric Materials – Synthesis, Characterization and Applications*, edited by Z. G. Ye (Woodhead, Cambridge, England, 2008), pp. 73–100.
[3]S. E. Park and T. R. Shrout, IEEE Trans. Ultrason. Ferroelectr. Freq. Control **44**, 1140 (1997).
[4]P. Sun, Q. Zhou, B. Zhu, D. Wu, C. Hu, J. M. Cannata, J. Tian, P. Han, G. Wang, and K. K. Shung, IEEE Trans. Ultrason. Ferroelectr. Freq. Control **56**(12), 2760 (2009).
[5]G. Gautschi, *Piezoelectric Sensorics* (Springer, Berlin, 2002).
[6]S. C. Woody, S. T. Smith, X. Jiang, and P. W. Rehrig, Rev. Sci. Instrum. **76**, 075112 (2005).
[7]X. Jiang, P. W. Rehrig, W. S. Hackenberger, E. Smith, S. Dong, D. Viehland, J. Moore, Jr., and B. Patrick, *Advanced Piezoelectric Single Crystal Based Actuators* (International Society for Optics and Photonics, 2005), pp. 253–262.
[8]D. Damjanovic, J. Am. Ceram. Soc. **88**, 2663 (2005).
[9]S. Zhang and F. Li, J. Appl. Phys. **111**, 031301 (2012).
[10]Y. Cho, S. Hashimoto, N. Odagawa, K. Tanaka, and Y. Hiranaga, Nanotechnology **17**(7), S137 (2006).
[11]Y. Lu, D. Y. Jeong, Z. Y. Cheng, Q. Zhang, H. S. Luo, Z. W. Yin, and D. Viehland, Appl. Phys. Lett. **78**(20), 3109 (2001).
[12]S. Wada, S. E. Park, L. E. Cross, and T. R. Shrout, Ferroelectrics **221**(1), 147 (1999).
[13]P. Zubko, N. Stucki, C. Lichtensteiger, and J. M. Triscone, Phys. Rev. Lett. **104**(18), 187601 (2010).
[14]R. Zhang, B. Jiang, and W. Cao, J. Appl. Phys. **90**(7), 3471 (2001).
[15]J. Tian, P. Han, X. Huang, H. Pan, J. F. Carroll, and D. A. Payne, Appl. Phys. Lett. **91**(22), 222903 (2007).
[16]S. E. Park and T. R. Shrout, J. Appl. Phys. **82**, 1804 (1997).
[17]D. Lin, S. Zhang, Z. Li, F. Li, Z. Xu, S. Wada, J. Luo, and T. R. Shrout, J. Appl. Phys. **110**(8), 084110 (2011).
[18]P. Urenski, M. Lesnykh, Y. Rosenwaks, G. Rosenman, and M. Molotskii, J. Appl. Phys. **90**, 1950 (2001).
[19]S. Wada, K. Yako, T. Muraishi, K. Yokoh, S. M. Nam, H. Kakemoto, and T. Tsurumi, Ferroelectrics **340**, 17 (2006).
[20]Y. J. Yamashita, N. Yamamoto, K. Itsumi, and Y. Hosono, Jpn. J. Appl. Phys. **50**, 09NC05 (2011).
[21]L. H. Peng, Y. C. Fang, and Y. C. Lin, Appl. Phys. Lett. **74**, 2070 (1999).
[22]V. Shur, E. Rumyantsev, R. Batchko, G. Miller, M. Fejer, and R. Byer, Ferroelectrics **221**, 157 (1999).
[23]R. G. Batchko, V. Y. Shur, M. M. Fejer, and R. L. Byer, Appl. Phys. Lett. **75**, 1673 (1999).
[24]V. Y. Shur, E. Rumyantsev, E. Nikolaeva, E. Shishkin, D. Fursov, R. Batchko, L. Eyres, M. Fejer, and R. Byer, Appl. Phys. Lett. **76**(2), 143 (2000).
[25]H. I. Smith, Physica E (Amsterdam) **11**(2), 104 (2001).
[26]Q. Xie, M. Hong, H. Tan, G. Chen, L. Shi, and T. Chong, J. Alloys Compd. **449**(1), 261 (2008).
[27]S. Zhang, S. M. Lee, D. H. Kim, H. Y. Lee, and T. R. Shrout, J. Am. Ceram. Soc. **91**(2), 683 (2008).
[28]V. Y. Shur, *Frontiers of Ferroelectricity* (Springer, 2007), pp. 199–210.
[29]M. Kohli, P. Muralt, and N. Setter, Appl. Phys. Lett. **72**(24), 3217 (1998).
[30]Y. Guo, H. Luo, K. Chen, H. Xu, X. Zhang, and Z. Yin, J. Appl. Phys. **92**(10), 6134 (2002).
[31]D. Viehland and Y. H. Chen, J. Appl. Phys. **88**(11), 6696 (2000).
[32]Z. Li, Z. Xu, X. Yao, and Z.-Y. Cheng, J. Appl. Phys. **104**, 024112 (2008).
[33]Y. Jin, Y. Wang, A. Khachaturyan, J. Li, and D. Viehland, Phys. Rev. Lett. **91**(19), 197601 (2003).